

Rotor Vibration Simulation Method for Active Magnetic Bearing Control

Osami MATSUSHITA, Mechanical Engineering Research Laboratory, Hitachi,
502, Kandatsu-machi, Tsuchiura-shi, Ibaraki-ken

Toyomi YOSHIDA, Mechanical Engineering Research Laboratory, Hitachi, Ltd.

Naohiko TAKAHASHI, Mechanical Engineering Research Laboratory, Hitachi, Ltd.

ABSTRACT Since active magnetic bearings have been employed in turbo-machinery, a corresponding simulation technique combined with rotor dynamics and controller network is required for design, tuning operations, and so on. This paper presents the simulation method and its applications to stability estimation, unbalance responses and frequency response of a servo control system.

The rotor system is reduced to a small model by a quasi-modal modeling we developed. The control network is expressed by the usual state equations. Both the model and the equations are then combined for the simulation analysis. In addition to the usual control law, e. g., PID, the observer based state feedback and so on, the developed program is capable to cover the tracking filter with rotational speed and cross talk between x and y channel control, which are related to empirical knowhow of the rotor vibration control.

Some examples of the numerical simulation are presented for demonstrating practical applications of the developed program.

1. INTRODUCTION

Rotordynamics related to ball and oil-film bearings have been the major subject in the study and development of rotor vibration analysis programs. Since present industrial rotating machines such as turbine compressors use passive bearings, such programs can cover almost all types of rotating machines.

Recently, however, electromagnetic bearings, i.e., active bearings, are increasingly used in various types of rotating machines. Currently available commercial control-type rotating machines incorporating electromagnetic bearings are mostly small-scale machines such as turbo molecular pumps and X-ray tubes. However, the application range is increasing to large-scale rotating machines as well.

Electromagnetic bearings are thus becoming more important in the field of rotating machines in general. As a result software to assist in the design and development of rotating machines controlled by electromagnetic bearings is being currently developed.

In the case of an electromagnetic bearing, the output current is determined by an electronic circuit on the basis of input of displacement signals detected and then runs through a coil and induces an electromagnetic force because of vibration restraint. All bearing reaction forces are determined by the electronic circuit according to control rules. Accordingly, the control system of the rotor must be analyzed from the viewpoint of both the conventional rotor dynamics and the control theory.

Rotor vibration is modeled by the quasi-modal method^[1], while the electronic circuit is expressed by a set of state equations. The problem is how to combine these two formulations. Rotor vibration is described as a lateral vibration consisting of forward and backward rotor motions. In accordance with this, the electronic circuit is represented as a transfer function, where backward transfer function $G(-j\omega)$ is used in addition to the ordinary forward transfer function $G(j\omega)$.

This study summarizes a method to combine the rotor and electronic circuit by introducing the concept of forward and backward vibration. Some examples are shown to demonstrate the suitability of the developed method for stability analysis, unbalance response analysis, and frequency response analysis.

MOMENCLATURES

- M : mass matrix
- C_g : gyroscopic effect matrix
- K : $= \begin{pmatrix} K_{11} & K_{12} \\ K_{21} & K_{22} \end{pmatrix}$ rotor stiffness matrix ($K_{21}^t = K_{12}$).
- F : $[F_1, F_2]$: force
- U_r, U_b : Unbalance vector
- Z : complex displacement vector
- ≡ : equal by definition
- ★ : conjugate of ★
- Q : bearing reaction force
- z₁ : displacement vector of inner coordinates
- z₂ : displacement vector of boundary coordinates
- ω : natural frequency of rotor inner system mode
- φ, φ_i, φ_b : undamped critical speed mode of inner system
- δ : deflection mode when boundary coordinates are forcedly displaced
- ξ : deflection mode when the boundary is forcedly displaced at unit speed
- Ω : rotational speed
- k₂* : equivalent spring constant at forced displacement of bearing
- C_{g2}* : equivalent gyroscopic action at forced speed of bearing
- S, S_i : quasi-modal coordinates
- G(s), H(s) : transfer functions
- i = imaginary unit = $\sqrt{-1}$
- B*₁₁ : modal mass corresponding to bending mode
- B*₁₂ : modal mass corresponding to relation between bending mode and bearing forced displacement and/or velocity

B_{22}^* : modal mass corresponding to bearing forced displacement

2. SYSTEM STRUCTURE OF A CONTROLLED TYPE ROTOR

2.1 Equation of Motion for Rotor System

Since the displacements x and y in directions X and Y of the rotor vibration are represented, the combination of both rotor vibrations is represented by a complex displacement $Z = x + iy^{[2]}$. Further, displacement of the boundary (the bearing) is denoted by Z_2 , and that of the other inner system of the rotor by Z_1 . Hereafter, the inner system is represented by suffix 1, and the boundary by suffix 2. Then, the equation of motion is obtained as follows:

$$\begin{pmatrix} M_1 \\ M_2 \end{pmatrix} \begin{pmatrix} \ddot{Z}_1 \\ \ddot{Z}_2 \end{pmatrix} + \begin{pmatrix} i\Omega C_{q1} \\ i\Omega C_{q2} \end{pmatrix} \begin{pmatrix} \dot{Z}_1 \\ \dot{Z}_2 \end{pmatrix} + \begin{pmatrix} K_{11} & K_{12} \\ K_{21} & K_{22} \end{pmatrix} \begin{pmatrix} Z_1 \\ Z_2 \end{pmatrix} = \begin{pmatrix} F_1 \\ F_2 \end{pmatrix} - \begin{pmatrix} 0 \\ Q \end{pmatrix} - \begin{pmatrix} 0 \\ G \end{pmatrix} \quad (1)$$

where F_1, F_2 ; force

$Q = Q(Z, \dot{Z}, \bar{Z}, \bar{\dot{Z}})$; reaction force of oil-film lubricated bearing

$G = G(j\omega) = G(Z, \dot{Z})$; reaction force of electromagnetic bearing

If the right side of Eq.(1) is represented by force F_A and written a simple form using complex displacement Z , we obtain:

$$M\ddot{Z} + i\Omega Cg\dot{Z} + KZ = F_A \quad (2)$$

From Eq.(2), a state equation is as follows:

$$\begin{pmatrix} M \\ K \end{pmatrix} \begin{pmatrix} \ddot{Z} \\ \dot{Z} \end{pmatrix} + \begin{pmatrix} -i\Omega Cg - K \\ K \quad 0 \end{pmatrix} \begin{pmatrix} \dot{Z} \\ Z \end{pmatrix} = \begin{pmatrix} F_A \\ 0 \end{pmatrix} \quad (3)$$

The following transformation is defined for the quasi-modal transformation shown in Fig.1:

$$\begin{pmatrix} \dot{Z}_1 \\ \dot{Z}_2 \\ Z_1 \\ Z_2 \end{pmatrix} = \begin{pmatrix} i\omega\phi & \delta & 0 \\ 0 & \mathbf{1} & 0 \\ \phi & \xi & \delta \\ 0 & 0 & \mathbf{1} \end{pmatrix} \begin{pmatrix} S_1 \\ S_2 \\ Z_2 \end{pmatrix} \equiv [\Phi] \begin{pmatrix} S_1 \\ Z_2 \end{pmatrix} \quad (4)$$

where $\mathbf{1} = [1, 1, \dots, 1]^t$.

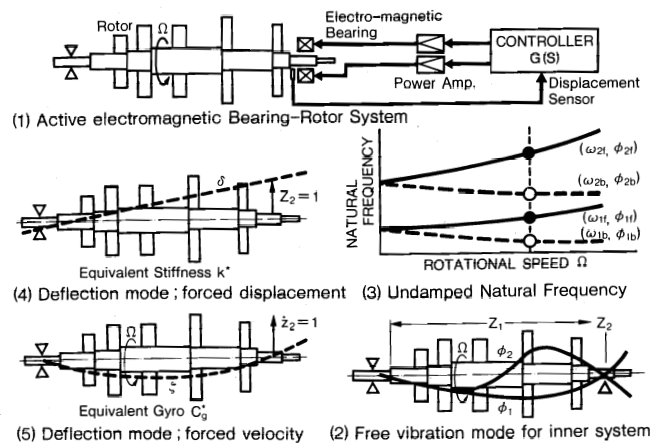


Fig.1 Mode Shapes for Quasi-modal Transformation

Substitute Eq.(4) in Eq.(3) and perform a conjugate transpose of $[\Phi]$ to obtain the following equation:

$$\begin{pmatrix} B_{11}^* & B_{12}^* & 0 \\ B_{12}^* & B_{22}^* & 0 \\ 0 & 0 & k_2^* \end{pmatrix} \begin{pmatrix} \dot{S}_1 \\ \dot{Z}_2 \\ \dot{Z}_2 \end{pmatrix} = \begin{pmatrix} i\omega B_{11}^* & 0 & 0 \\ 0 & -i\Omega C_{q2}^* & -k_2^* \\ 0 & k_2^* & 0 \end{pmatrix} \begin{pmatrix} S_1 \\ Z_2 \\ Z_2 \end{pmatrix} + \begin{pmatrix} -i\omega\phi^t F_1 \\ \delta^t F_1 + F_2 - Q - G \\ 0 \end{pmatrix} \quad (5)$$

where

$$B_{11}^* = \omega^2 \phi^t M_1 \phi + \phi^t K_{11} \phi$$

$$B_{12}^* = -i[\omega\phi^t M_1 \delta + \Omega\phi^t C_{q1} \delta]$$

$$B_{22}^* = \delta^t M_1 \delta + M_2 - \Omega^2 \xi \xi^t C_{q1} \delta$$

$$k_2^* = k_{21} \delta + k_{22}$$

= equivalent spring constant where inner system is viewed from the boundary

$$C_{q2}^* = k_{21} \xi \xi^t + C_{q2}$$

= equivalent damping factor where inner system is viewed from the boundary

Eq.(5) is the formulation for the portion which corresponds to the rotor system of a controlled type rotating machine. It represents the reduction by a quasi-modal transformation by the use of the eigenmode (marks \circ and \bullet) of the inner system at a certain rotational speed, as shown in Fig.1(3).

2.2 Dynamic Characteristics of Oil-Film Lubricated Bearings

In the case of a passive oil-film lubricated bearing, the bearing reaction forces Q_x and Q_y in directions X and Y , respectively, are represented by spring constants k_{ij} ($i, j = x, y$) and damping factors c_{ij} ($i, j = x, y$), and are defined as 8 parameters of oil-film as follows:

$$\begin{aligned} Q_x &= k_{xx}x + k_{yy}y + c_{xx}\dot{x} + c_{yy}\dot{y} \\ Q_y &= k_{yx}x + k_{xy}y + c_{yx}\dot{x} + c_{xy}\dot{y} \end{aligned} \quad (6)$$

It is generally known that the presence of cross stiffness such as k_{xy} and k_{yx} can cause unstable rotor vibrations.

2.3 Dynamic Characteristics of Electromagnetic Bearings

In the case of an active electromagnetic bearing. These dynamic factors are determined by the adjustment of the controller. Generally, isotropic dynamic characteristics of bearings are obtainable by adjustment:

$$k_d = k_{xx} = k_{yy} \quad c_d = c_{xx} = c_{yy}$$

$$k_c = k_{xy} = -k_{yx} \quad c_c = c_{xy} = -c_{yx}$$

Reaction forces are then given by the following equations:

$$\begin{aligned} Q_x &= k_d x + k_c y + c_d \dot{x} + c_c \dot{y} \\ Q_y &= k_c x - k_d y + c_c \dot{x} - c_d \dot{y} \\ \text{i. e. } Q &= Q_x + iQ_y \\ &= k_d z - ik_c z + c_d \dot{z} - ic_c \dot{z} \end{aligned} \quad (7)$$

Parameter k_c is an important factor in terms of stability. It indicates a cross talk between channels X and Y of the control circuit.

Generally, a controller accepts displacements x and y as input as shown in Fig.2, and consists of directly coupled transfer function $G_d(s)$ and of cross-coupled transfer function $G_c(s)$. As a result, forces Q_x and Q_y , in directions X and Y , respectively, are output via the actuator. Physically, this type of a system is a 2-input, 2-output type system. In the simulation, this form is transformed into 1-input,1-output type as shown below, by using a complex number.

$$Q = (G_d - iG_c)Z \tag{8}$$

Therefore, the problem is reduced to analysis of a control circuit system with one input ($Z = x + iy$) and one output ($Q = O_x + iQ_y$), with a complex transfer function $G(s) = G_d(d) - iG_c(s)$.

A control circuit can also be shown as follows using a state equation and an output equation:

$$\begin{aligned} B\dot{V} &= AV + RinZ \\ Q &= RoutV + DZ \end{aligned} \tag{9}$$

- B, A : factor matrix
- Rin : vector proportional to input
- Rout : vector proportional to output
- D : stiffness

where V is the voltage expressed in the complex form, $V = V_x + iV_y$, and V_x and V_y are voltages of the control circuit in directions X and Y , respectively.

3. STABILITY ANALYSIS

For the rotor system, the mode shown in Fig.1 is used to formulate a reduction system using the quasi-modal method. The control circuit is shown by a state equation. Stability analysis is actually performed by introducing a differential equation combining above two and by conducting a complex eigenvalue analysis for the equation.

The equation for a global system consisting of a quasi-modal reduced rotor system and control system be expressed as a matrix shown in Fig.3. From the upper left to the lower right corner of the

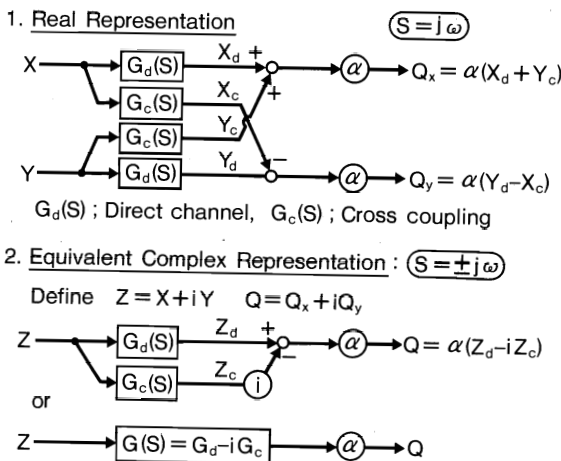


Fig.2 Network with X&Y Cross Coupling

matrix, the terms along the diagonal are vibration of the inner system of the rotor, vibration of electromagnetic bearing, and voltage of the control circuit.

The inner system starts to vibrate due to the presence of B_{21} . Through the vibration of the bearing, RIN is the bearing vibration, which is an input to the control circuit, while ROUT indicates the effects of reaction forces of the electromagnetic bearing, which the output of the control circuit.

4. UNBALANCE RESPONSE ANALYSIS^[3]

Unbalance response of rotors which are supported by oil-film lubricated bearings has been studied for many years. In this Section, contains discussion of the problem of definition of definition of the bearing characteristics when an oil-film lubricated bearing is replaced by an electromagnetic bearing.

4.1 Oil-Film Lubricated Bearing

Generally, the equation of motion for a rotor supported by oil-film lubricated bearings is given as follows:

$$M\ddot{Z} + i\Omega C_g \dot{Z} + KZ + Q = F = U\Omega^2 e^{i\Omega t} \tag{10}$$

Assume the vibration response and the bearing reaction force are given as follows :

$$Z = Z_f e^{i\Omega t} + \bar{Z}_b e^{-i\Omega t} \tag{11}$$

$$Q = Q_f e^{i\Omega t} + \bar{Q}_b e^{-i\Omega t} \tag{12}$$

Then, forward and backward vibration equations are obtained as follows:

$$\begin{aligned} [-\Omega^2(M + C_g) + K] Z_f + Q_f &= \Omega^2 U \\ Q_b + [-\Omega^2(M - C_g) + K] Z_b &= 0 \end{aligned} \tag{13}$$

If the following 8 parameters are used:

$$k_{xx} \quad k_{yy} \quad k_{xy} \quad k_{yx} \quad c_{xx} \quad c_{yy} \quad c_{xy} \quad c_{yx}$$

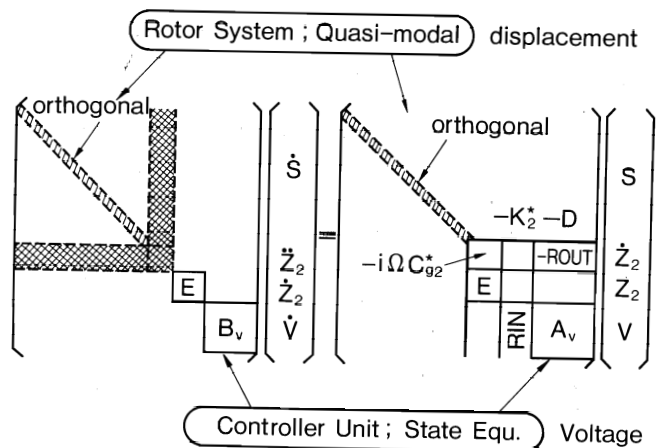


Fig.3 Global State Equation Combining Quasi-modal reduced Rotor with Controller

the characteristics of an oil-film lubricated bearing using complex forms are as follows:

$$K_f = \frac{K_{xx} + K_{yy}}{2} + i \frac{K_{yx} - K_{xy}}{2}, K_b = \frac{K_{xx} - K_{yy}}{2} + i \frac{K_{yx} + K_{xy}}{2}$$

$$C_f = \frac{C_{xx} + C_{yy}}{2} + i \frac{C_{yx} - C_{xy}}{2}, C_b = \frac{C_{xx} - C_{yy}}{2} + i \frac{C_{yx} + C_{xy}}{2}$$

Then, the bearing reaction force Q can be expressed as follows:

$$Q \equiv K_f \dot{z} + K_b \ddot{z} + C_f \dot{z} + C_b \ddot{z} \quad (14)$$

From Eq. (11), this relation becomes:

$$Q_f = (K_f + i\Omega C_f) Z_f + (K_b + i\Omega C_b) Z_b \quad (15)$$

$$Q_b = (\bar{K}_f + i\Omega \bar{C}_f) Z_b + (\bar{K}_b + i\Omega \bar{C}_b) Z_f$$

Finally, the following forward and backward vibration equations are obtained:

$$\left[(M + C_g) - \frac{K}{\Omega^2} - \frac{K_f + i\Omega C_f}{\Omega^2} \right] Z_f - \frac{K_b + i\Omega C_b}{\Omega^2} Z_b = -U \quad (16)$$

$$-\frac{K_b + i\Omega C_b}{\Omega^2} Z_f + \left[(M - C_g) - \frac{K}{\Omega^2} - \frac{K_f + i\Omega C_f}{\Omega^2} \right] Z_b = 0$$

If the vibration force is proportional to the rotational speed the following equation results:

$$F = U_f e^{i\Omega t} + \bar{U}_b e^{-i\Omega t} \quad (17)$$

This equation can be solved in a similar manner.

The rotor portion of Equ. (16) is analyzed using a structure shown in Fig. 5, where the quasi-modal transformation has been performed

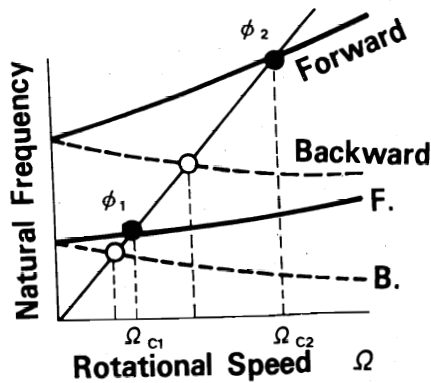


Fig. 4 Undamped Critical Speed (Inner System Only)

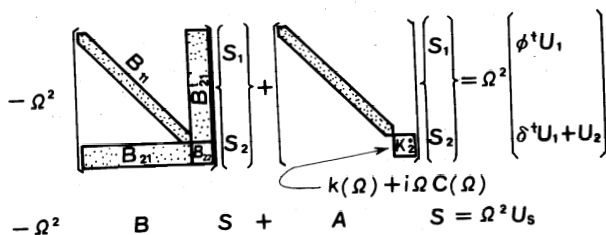
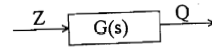


Fig. 5 Unbalance Response after Quasi-Modal Transformation

using orthogonality of the critical mode of the inner system shown in Fig. 4.

4.2 Electromagnetic Bearing

Transfer function of the electronic circuit of a controller for electromagnetic bearing is represented by $G(s)$. Displacement z is the input, and bearing reaction force Q is the output. This relationship can be shown in the following block diagram:



If input Z and output Q are as shown by Eq. (11) and (12), respectively, the following equations are obtained when $G(s)$ is a linear system:

$$Q_f = G(i\Omega) Z_f \quad (18)$$

$$Q_b = \bar{G}(-i\Omega) Z_b$$

By substituting the above in Eq. (13), the dynamic characteristics of electromagnetic bearings can be shown as follows:

$$K_f + i\Omega C_f = G(i\Omega), \quad K_b + i\Omega C_b = 0 \quad (19)$$

$$\bar{K}_f + i\Omega \bar{C}_f = \bar{G}(-i\Omega), \quad \bar{K}_b + i\Omega \bar{C}_b = 0$$

Eq. (16), which is applicable to oil-film lubricated bearings, is then rewritten to suit the case of the electromagnetic bearing using the above equation, and we obtain:

$$\left[(M + C_g) - \frac{K}{\Omega^2} - \frac{G(i\Omega)}{\Omega^2} \right] Z_f = -u \quad (20)$$

$$\left[(M - C_g) - \frac{K}{\Omega^2} - \frac{\bar{G}(-i\Omega)}{\Omega^2} \right] Z_b = 0$$

In this way, an unbalance response analysis can be performed using the quasi-modal modal, Fig. 5.

5. FREQUENCY RESPONSE ANALYSIS

Frequency response assumes inputting the electrical input E_n (n for nodal point) as a force. The matrix of a global system consisting of a rotor and a control circuit system is shown in Fig. 6. The upper half of the figure corresponds to the equation for the rotor system, and the lower half to the state equation for the control circuit system. f_n is a force working on the state equation, and includes E_n in its internal

$$i v \begin{bmatrix} B_{11}^* & B_{12}^* & 0 & 0 \\ B_{12}^{*T} & B_{22}^* & 0 & 0 \\ 0 & 0 & E & 0 \\ 0 & 0 & 0 & B \end{bmatrix} \begin{bmatrix} S_1 \\ \dot{z}_2 \\ Z_2 \\ v \end{bmatrix} = \begin{bmatrix} i\omega B_1^* & 0 & 0 & 0 \\ 0 & -i\Omega C_{g2}^* - K_2^* - D_1^* & -R_{out} & 0 \\ 0 & E & 0 & 0 \\ 0 & 0 & R_{in} & A \end{bmatrix} \begin{bmatrix} S_1 \\ \dot{z}_2 \\ Z_2 \\ v \end{bmatrix} + \begin{bmatrix} 0 \\ f_n \\ 0 \\ f_n \end{bmatrix}$$

where,

$$B_{11}^* = \omega^2 \phi^T M_1 \phi + \phi^T K_{11} \phi, \quad \phi = \text{diagonal matrix} \quad K_2^* = k_{21} \delta + k_{22}$$

$$B_{12}^* = -i \omega \phi^T M_1 \delta + \Omega \phi^T C_{g1} \delta \quad C_{g2}^* = k_{21} \epsilon_g + C_{g2}$$

$$B_{22}^* = \delta^T M_1 \delta + M_2 - \Omega^2 \epsilon_g^T C_{g1} \delta \quad \epsilon = i\Omega \epsilon_g$$

Fig. 6 Matrix Structure for Global System (Frequency Response Analysis)

portion.

The force, which is obtained from the output equation of the control circuit system, works as a reaction force to suppress the bearing vibration. For this reason, the portion corresponding to the bearing vibration has a minus sign as shown in Fig.6, before it is stored.

6. EXAMPLES OF NUMERICAL CALCULATION

6.1 Basic Characteristics of Analysis Model

The vertical rotor, shown in Fig.7, was used as the analysis model. A high frequency motor (No. 20) was located between the upper and lower electromagnetic bearings (No. 13 and 28). Thrust bearings were used for the rotor shaft.

To identify the basic characteristics of this rotor, the upper and lower electromagnetic bearings are replaced by spring constants, which are then used as parameters for indicating change in the natural frequency. The results are shown in Fig.8. The horizontal axis shows bearing stiffness, and the vertical axis shows frequencies. The frequencies shown are, from bottom up, 1st and 2nd rigid modes and 1st, 2nd, and 3rd bending modes. The shape of each mode is shown in the lower right corner of the figure.

Since the rated speed of this particular rotor is 300rps, the modes up to the 1st bending mode are covered in the control range, as seen in Fig.8. It is now necessary to adjust so that the 2nd bending mode and higher nodes will not vibrate.

The block diagram of a control circuit is shown in Fig.9. The basic structure comprises a PID circuit with proportional, integral and differential elements. In addition to the PID circuit, a notch filter and a low pass filter with cross stiffness are provided to stabilize the high and low frequency modes, respectively. Further, a tracking filter with cross stiffness is used to prevent resonance.

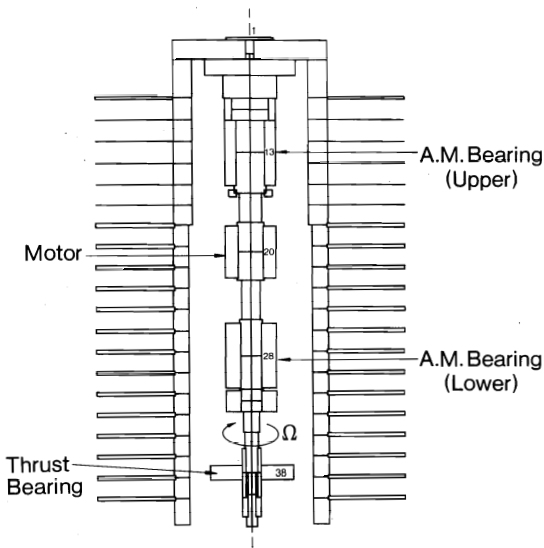


Fig.7 Calculation model

Simulations to rotate the rotor suitably up to the rated speed by using the added portions are performed. The results are discussed below.

6.2 Stabilization of High Frequency Mode

First, stabilization of high frequency mode is described referring to Fig.10. The Bode diagram of transfer characteristics of the PID circuit proper is shown in the upper part of Fig.10. The horizontal axis is for frequencies and the vertical axis for gain and phase. Regarding the phase, the hatched area indicates the phase-advance area, or generally stable area.

If the rotor is rotated using this PID circuit, higher modes (2nd and 3rd bending modes) enter the phase-delay area when the rotor reaches a certain rotational speed resulting in unstable operation. A notch filter was incorporated and the phase-advance area was enlarged in order to stabilize these modes. Cases 1 through 4 in Fig.10 indicate this process, and simply show the phase-advance and phase delay areas.

In case 1, the poles of the notch filter were set at 350Hz ($\zeta = 0.1$)

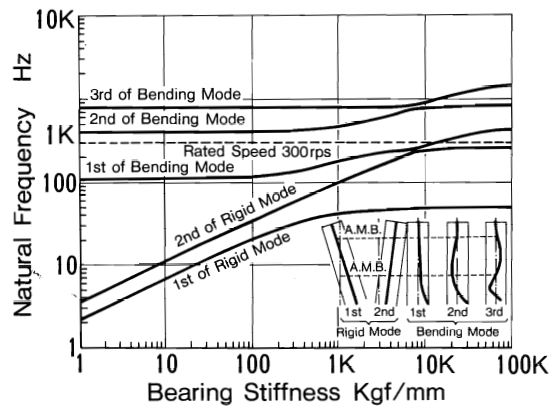


Fig.8 Relationship of natural frequency versus bearing stiffness

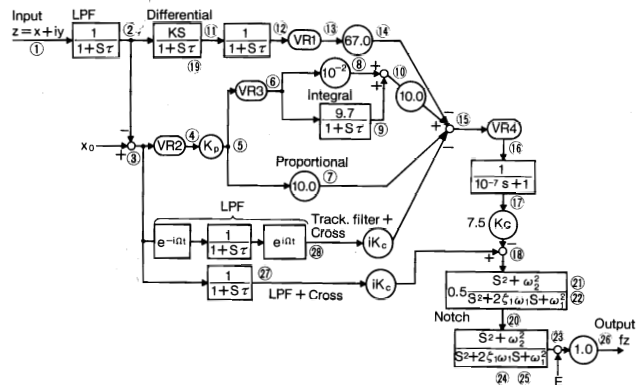


Fig.9 Network of controller (PID + Notch filter, LPF + Cross, Track. filter + Cross)

and 680Hz ($\zeta = 0.1$). The phase-advance area was not large enough, and the modes of 346Hz and 954Hz were unstable. In cases 2 and 3 unstable modes were also observed. The range where all eigenvalues up to the rated speed would move was checked, and the frequency and damping ratio of the notch filter were adjusted so that the filter would cover all of these eigenvalues. As a result, the high frequency mode was stabilized as shown in case 4. Transfer characteristics of the control circuit proper in this instance are summarized in the Bode diagram shown in the bottom part of Fig.10.

6.3 Stabilization of Low Frequency Mode

Fig.11 shows the results of stability analysis made with the use of the PID circuit equipped with a notch filter and adjusted as discussed in Section 6.2. Rotational speed is shown in relation to the horizontal axis. The figure on the left side indicates the change in the each eigenvalue, while the figure on the right side shows the change in the damping ratio. The solid lines are for forward and the dashed lines for the backward mode. The first backward mode is unstable for rotational speed over 200 rps, as shown in the figure. To stabilize the mode, a low pass filter with cross stiffness was added to the control circuit. As a result of parameter adjustment, the first backward mode was improved as indicated by the dashed line pointed by the arrow, and the mode was now stable throughout the range of the rated speed.

6.4 Resonance Prevention

An example of unbalance response calculation is shown in Fig.12.

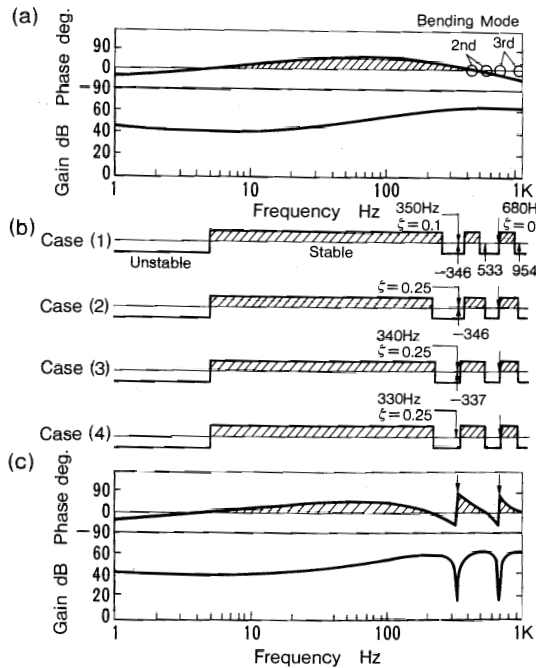


Fig.10 Stabilization of High Frequency Modes (Notch filter)

The horizontal axis is for rotational speed, against which the change in amplitude is shown. Unbalance quantities are shown in the figure. From this example, it is deduced that although the peak of the first bending mode appears around 170 rps, amplitude can be held at a low level by adjusting the value of tracking cross stiffness.

6.5 Frequency Response Analysis

Lastly Fig.13 shows a complete round of transfer characteristics obtained for the global system comprising the rotor and control circuit system. The figure shows the open loop characteristics of the lower rotor shaft. The horizontal axis is for frequency, as a function of which the change in gain and phase is shown. This example is for rotor speed of 0 rps. Generally, in a gain curve, the peak of the resonant point represents the eigenmode when the electromagnetic bearing is free, while the peak of the antiresonant point does so when the bearing is pin-fixed.

Fig.14 shows the open loop characteristics for rotor speed of 300 rps. Since these two examples are for the forward vibration, the position of the gain peak is moving toward the higher frequencies as the rotational speed increases.

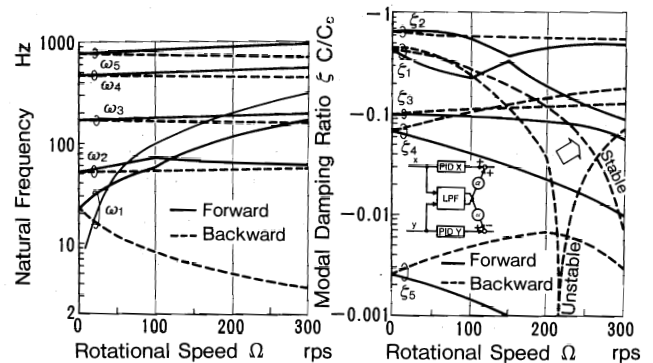


Fig.11 Stability Analysis (LPF + Cross Stiffness)

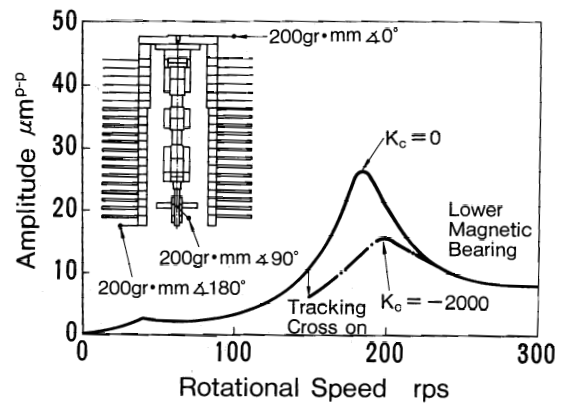


Fig.12 Unbalance Response and Cross Coupling Effect (Tracking filter + Cross Stiffness)

7. CONCLUSIONS

The above contents is summarized as follow.

- (1) For the turning vibration of a rotor, forward transfer function $G(j\omega)$ and backward transfer function $G(-j\omega)$ were introduced in the electronic circuit, and a differential equation was established to couple the rotor and the electronic circuit.
- (2) It is possible to analyze a cross circuit and tracking/tuning type circuit by expressing the transfer function $G(s)$ of electronic circuit with a complex number.
- (3) A force may be input at any desired point because the rotor system and electronic circuit system are meshed and assigned with nodal points by the finite element method. Further, output points may be freely changed to obtain transfer characteristics, because a sensor can be installed on any desired point.
- (4) Stability analysis, unbalance response analysis and frequency response analysis were explained using examples.

8. REFERENCES

- [1] O. Matsushita, et al 2;
Trans. of JSME Vol 48, No. 431C, (1982), p. 925 (in Japanese)
- [2] O. Matsushita, et al 2;
Trans. of JSME Vol 47, No. 418C, (1981), p. 727 (in Japanese)
- [3] O. Matsushita and M. Ida;
Trans. of JSME Vol 50, No. 452C, (1984), p. 626 (in Japanese)
- [4] H. Saito;
Mechanical Vibration in Engineering, chapter 8, Yokendo (1982) (in Japanese)

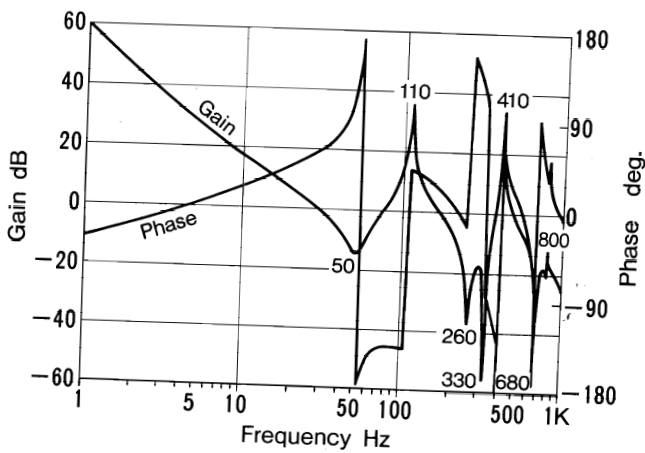


Fig.13 Overall transfer function (Lower X) 0rps

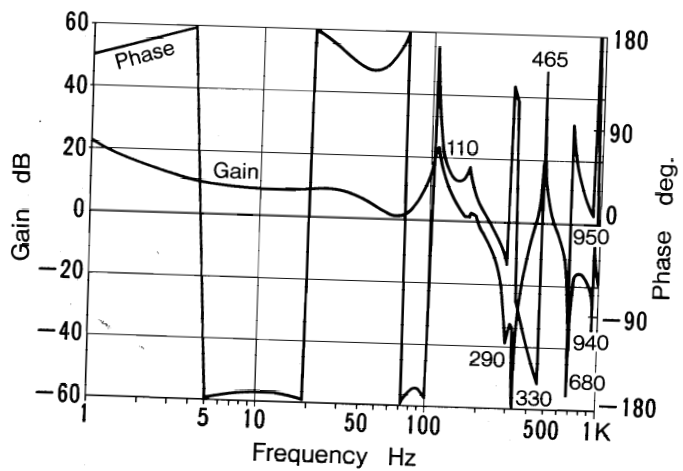


Fig.14 Overall transfer function (Lower X) 300rps

